

Evidence of rapid phenocryst growth of olivine during ascent in basalts from the Big Pine volcanic field: Application of olivine-melt thermometry and hygrometry at the liquidus

¹S.K. Brehm and ¹R.A. Lange

¹Department of Earth and Environmental Sciences, University of Michigan, 2534 North University Building, 1100 North University Avenue, Ann Arbor, Michigan 48109-1005, USA

Contents of this file

Calculation of minimum ascent rates

Figure S1. Image of BP-11 mantle xenolith

Figure S2. Chondrite-normalized trace-element diagram of BP basalts

Figure S3. Plots of Na₂O vs Mg# and TiO₂ vs Mg# in clinopyroxene for BP-24 and BP-7

Figure S4. Histograms of anorthite content in the four low-MgO BP basalts and application of plagioclase-liquid hygrometer

Table S1. Analyzed trace element concentrations for all ten BP samples

Table S2. Measured FeO wt% from titrations using the Wilson (1960) method

Table S3. Standards employed for electron microprobe analyses of olivine, clinopyroxene, plagioclase, and Fe-Ti oxides

Additional Supporting Information (Files uploaded separately)

Table S4. Olivine phenocryst analyses for ten BP basalts

Table S5 Clinopyroxene analyses for six high-MgO BP basalts

Table S6. Plagioclase phenocryst analyses for four BP basalts

Table S7. Ilmenite and titanomagnetite analyses for BP-20

Introduction

This file contains a detailed description of estimates of minimum ascent rates using Stoke's settling law. The four supplementary figures and three supplementary tables in this file are those that may be of interest to many readers, but are not essential information for the main text.

Figures S1, S2, S3, S4

The figures include a photograph of the mantle xenolith in sample BP-11 (Fig. S1), a chondrite-normalized trace-element plot of the BP basalts (Fig. S2), a plot of clinopyroxene analyses for two additional basalt samples (BP-24 and BP-7) that complement Figure 7 in the main text (Fig. S3), and histograms of plagioclase analyses obtained in each of the four low-MgO BP basalts (Fig. S4). All information about how the microprobe data were collected for Figure S3 and S4 is found in the main text.

Tables S1, S2, S3

The tables include a compilation of all analyzed trace elements for the ten BP basalts (ICP-MS analyses from Actlabs (Canada) in this study (Table S1), the two sets of analyses of wt% FeO in all ten BP basalts and certified standard using the titration method of Wilson (1960) (Table S2), and a list of the microprobe standards used for mineral analyses at the University of Michigan (Table S3).

Tables S4, S5, S6, S7

The four remaining supplementary tables provide all microprobe mineral analyses obtained in this study for olivine (Table S4), clinopyroxene (Table S5), plagioclase (Table S6) and Fe-Ti oxides (Table S7). Because they are each multi-paged, they are uploaded individually. All details about how data were obtained are described in the main text.

Calculation of minimum ascent rates

For a mantle xenolith to be carried to the surface, the ascent velocity of the host basalt must be sufficiently rapid to overcome the settling velocity of the mantle xenolith. For a Newtonian fluid, the minimum ascent velocity for a mantle xenolith can be approximated using Stoke's law:

$$v = \frac{2gr^2(\rho_{\text{xenolith}} - \rho_{\text{liquid}})}{9\eta} \quad (1)$$

In the expression above, g is the gravitational acceleration (9.8 ms^{-2}), ρ is density (g/cm^3), and η is the viscosity of the liquid (Pa s). However, Sparks et al. (1977) and Spera (1980, 1984) caution that the Stoke's calculation presented in Equation 1 may be an oversimplification as it assumes the melt is Newtonian. The melt may instead behave like a Bingham fluid, in which case crystal abundance must be accounted for. Therefore, the calculated minimum ascent velocities presented below are between the depth of melt segregation and the onset of phenocryst growth, when phenocrysts are not present.

Equation (1) is used to calculate the minimum ascent velocity of the basalt (BP-11) that hosted the mantle xenolith (2 cm radius) found in this study. Previous work has shown that the Big Pine mantle xenoliths are predominantly spinel lherzolites (e.g., Wilshire et al., 1988; Beard & Glazner, 1995; Lee, 2001), which have an approximate average density of 3.3 g/cm^3 (e.g. Spera, 1980). The whole-rock composition of BP-11 (Table 1) is used to calculate the liquid density and viscosity at 1200°C . Previous work on olivine-hosted melt inclusions has shown that BP basalts contain between 1.5 and 3.0 wt% H_2O (Gazel et al., 2012), thus the density and viscosity of BP-11 is calculated using both values. The density of the liquid is calculated according to the model of Lange and Carmichael (1990), Lange (1997), and Ochs and Lange (1999), and the viscosity of the liquid is calculated using the model of Hui and Zhang (2007). The calculations give a minimum ascent velocity of 0.07-0.28 m/s (5.8 and 23.8 km/day), respectively, for BP-11 with 1.5 and 3.0 wt% H_2O .

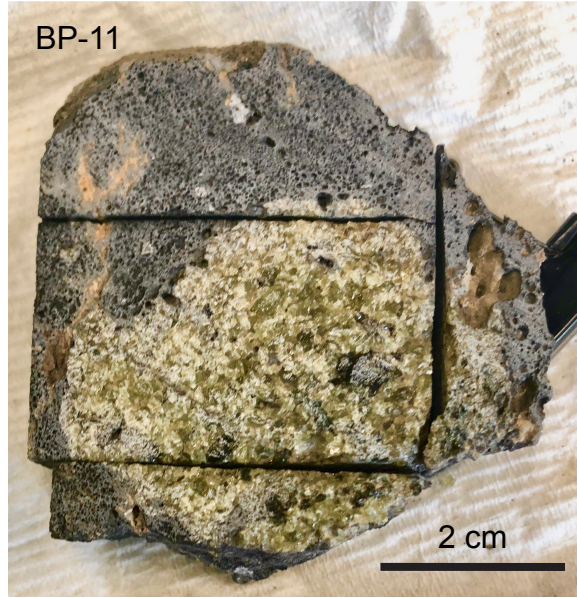


Figure S1. Mantle xenolith found in sample BP-11.

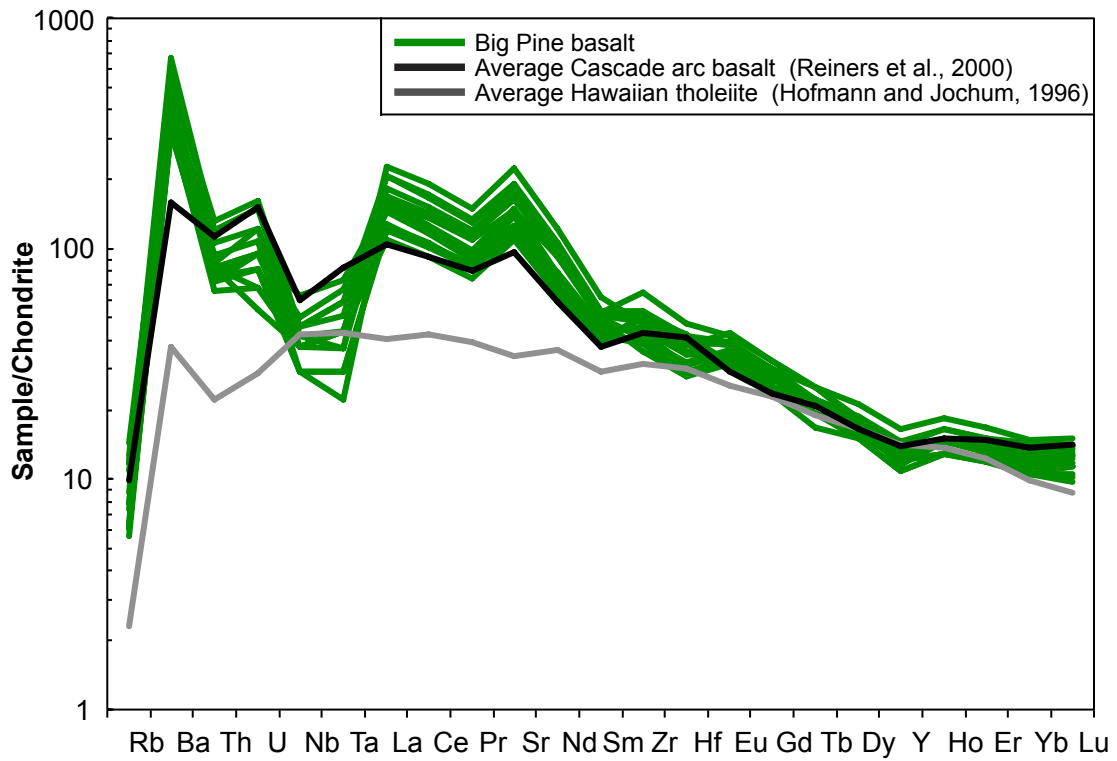


Figure S2. Chondrite-normalized (McDonough & Sun, 1995) trace-element diagram of the BP basalts compared to average Cascade arc basalt (Reiners et al., 2000) and an average Hawaiian tholeiite (Hofmann & Jochum, 1996).

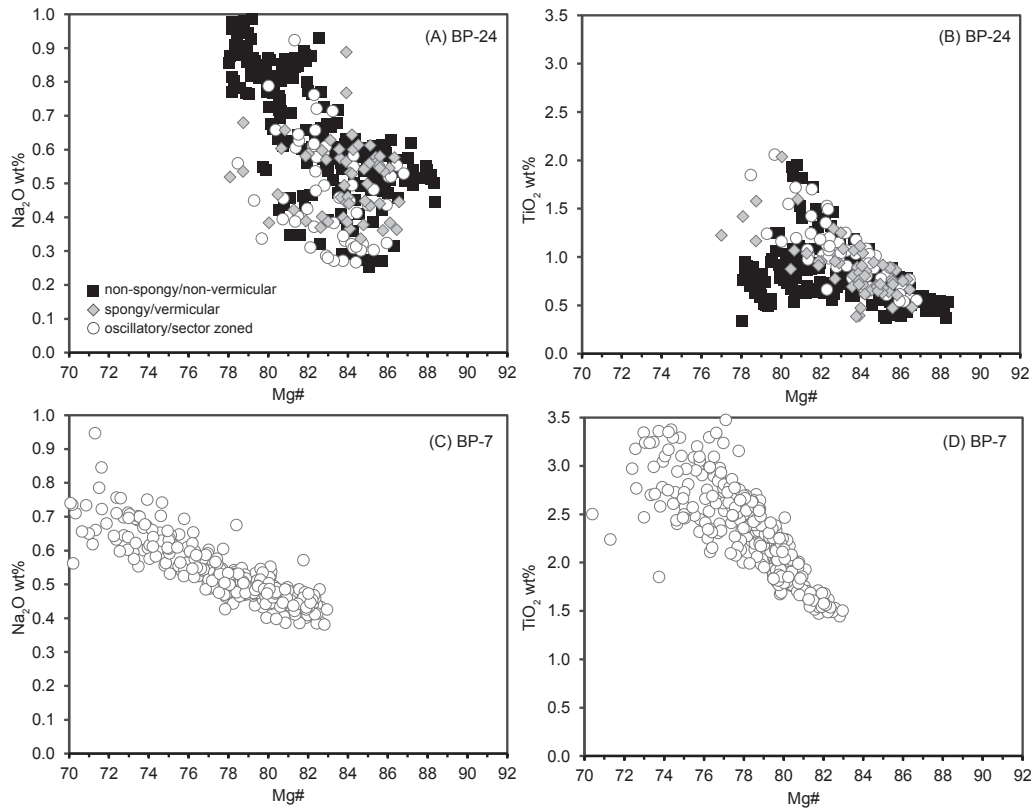


Figure S3. Plots of Na₂O vs Mg# (left) and TiO₂ vs Mg# (right) in clinopyroxene crystals from two high-MgO BP basalts (BP-24, BP-7) not shown in Figure 7 of main paper. Analyses are given different symbols based on clinopyroxene textures including non-spongy (non-vermicular), spongy (vermicular), and sector- or oscillatory-zoned crystals. The results for BP-24 are broadly similar to those for the samples in Figure 7, whereas those for BP-7 are based on sector-zoned microlites in groundmass (only occurrence of clinopyroxene in this sample).

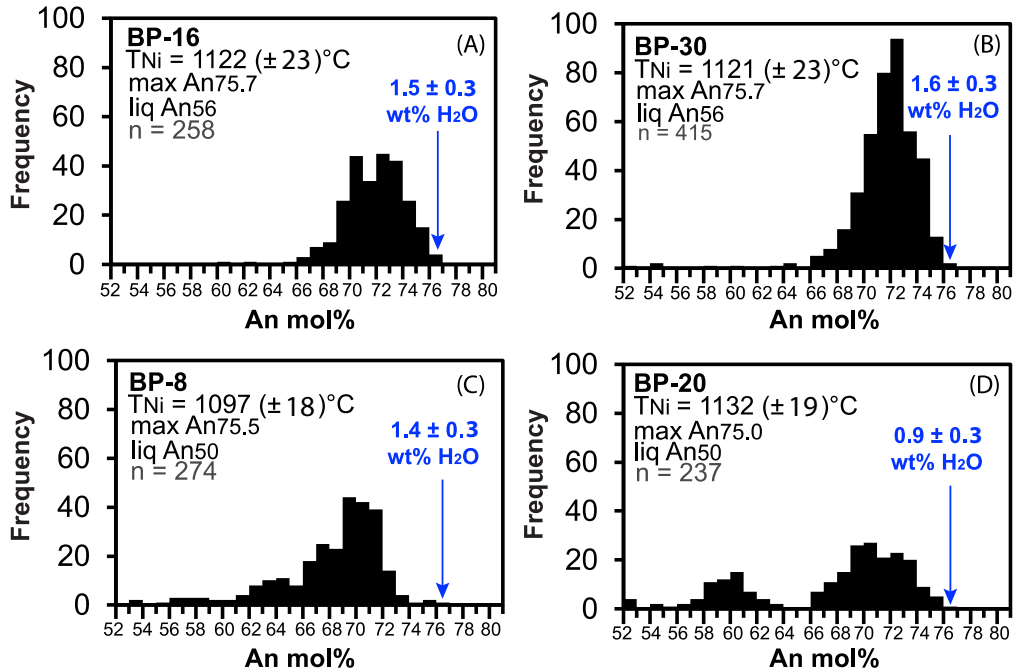


Figure S4. Histograms of anorthite content ($An\ mol\% = (X_{CaO}/(X_{CaO} + X_{Na2O} + X_{K2O}) \times 100)$) for analyzed plagioclase in four BP basalts. The composition of the most An-rich plagioclase in each sample is reported in Table S6. The most An-rich plagioclase composition, whole-rock composition, and T_{Ni} in each sample are used to calculate the minimum H₂O wt% (see main text) using the plagioclase-liquid hygrometer (Waters & Lange, 2015). The most calcic plagioclase composition (An mol%), liquid An number, T_{Ni} , minimum H₂O wt%, and number of analyses (=n) are given for each sample.

Table S1. Analyzed trace element concentrations for 10 BPVF samples

(ppm)	BP-23	BP-31	BP-11	BP-19	BP-24	BP-7	BP-16	BP-30	BP-8	BP-20
Sc	28	32	26	28	25	25	28	28	25	24
Be	<i>b.d</i>	<i>b.d</i>	<i>b.d</i>	<i>b.d</i>	<i>b.d</i>	<i>b.d</i>	<i>b.d</i>	<i>b.d</i>	<i>b.d</i>	<i>b.d</i>
V	201	231	211	243	208	196	223	223	186	190
Cr	740	700	350	330	330	280	80	70	190	200
Co	75	90	108	75	76	70	94	67	58	77
Ni	343	265	212	168	208	198	88	88	107	114
Zn	54	54	59	56	56	91	67	68	58	58
Cd	<i>b.d</i>	<i>b.d</i>	<i>b.d</i>	<i>b.d</i>	<i>b.d</i>	<i>b.d</i>	<i>b.d</i>	<i>b.d</i>	<i>b.d</i>	<i>b.d</i>
S	0.006	0.009	0.006	0.006	0.006	0.004	0.004	0.017	0.003	0.003
Cu	52	56	50	48	48	125	54	66	34	42
Ag	<i>b.d</i>	<i>b.d</i>	<i>b.d</i>	<i>b.d</i>	<i>b.d</i>	<i>b.d</i>	<i>b.d</i>	<i>b.d</i>	<i>b.d</i>	<i>b.d</i>
Pb	<i>b.d</i>	<i>b.d</i>	<i>b.d</i>	<i>b.d</i>	<i>b.d</i>	<i>b.d</i>	<i>b.d</i>	<i>b.d</i>	<i>b.d</i>	<i>b.d</i>
Ga	15	15	17	17	17	17	19	19	18	18
Ge	<i>b.d</i>	<i>b.d</i>	<i>b.d</i>	<i>b.d</i>	<i>b.d</i>	<i>b.d</i>	<i>b.d</i>	<i>b.d</i>	<i>b.d</i>	<i>b.d</i>
As	<i>b.d</i>	<i>b.d</i>	<i>b.d</i>	<i>b.d</i>	<i>b.d</i>	<i>b.d</i>	<i>b.d</i>	<i>b.d</i>	<i>b.d</i>	<i>b.d</i>
Rb	14	18	27	27	29	20	15	14	25	27
Sr	1293	1181	1382	1612	1329	1067	899	891	824	795
Y	19	19	22	21	20	26	23	22	22	21
Zr	136	155	206	182	192	246	171	176	194	193
Nb	7	9	11	10	11	15	7	7	9	9
Mo	<i>b.d</i>	<i>b.d</i>	<i>b.d</i>	<i>b.d</i>	<i>b.d</i>	<i>b.d</i>	<i>b.d</i>	<i>b.d</i>	<i>b.d</i>	<i>b.d</i>
In	<i>b.d</i>	<i>b.d</i>	<i>b.d</i>	<i>b.d</i>	<i>b.d</i>	<i>b.d</i>	<i>b.d</i>	<i>b.d</i>	<i>b.d</i>	<i>b.d</i>
Sn	<i>b.d</i>	<i>b.d</i>	<i>b.d</i>	<i>b.d</i>	<i>b.d</i>	<i>b.d</i>	<i>b.d</i>	<i>b.d</i>	<i>b.d</i>	<i>b.d</i>
Sb	<i>b.d</i>	<i>b.d</i>	<i>b.d</i>	<i>b.d</i>	<i>b.d</i>	<i>b.d</i>	<i>b.d</i>	<i>b.d</i>	<i>b.d</i>	<i>b.d</i>
Cs	<i>b.d</i>	<i>b.d</i>	<i>b.d</i>	<i>b.d</i>	<i>b.d</i>	<i>b.d</i>	<i>b.d</i>	<i>b.d</i>	<i>b.d</i>	<i>b.d</i>
Ba	1031	1159	1338	1627	1301	820	788	773	827	817
La	40.1	39.1	49.2	53.9	49.2	37	29	28.6	30	25.8
Ce	87.2	86.4	105	117	102	83.4	64.2	62.3	65.3	56.4
Pr	10.4	10.6	12.4	13.9	12.1	10.2	7.9	7.65	7.72	6.93
Nd	42.3	43	48.8	55.5	47.4	42	33.2	32.1	31.3	28.9
Sm	7.2	7.5	7.9	9.1	7.8	7.8	6.6	6.4	5.8	5.8
Eu	2.03	2.05	2.22	2.42	2.16	2.34	1.94	1.91	1.8	1.68
Gd	5.6	5.6	6	6.5	6	6.5	5.7	5.4	5.5	5
Tb	0.7	0.7	0.9	0.9	0.8	0.9	0.8	0.8	0.8	0.8
Dy	4	3.9	4.5	4.4	4.3	5.2	4.6	4.5	4.6	4.2
Ho	0.7	0.7	0.8	0.8	0.8	1	0.9	0.8	0.9	0.8
Er	1.9	2	2.3	2.3	2.2	2.7	2.4	2.3	2.4	2.1
Tm	0.26	0.27	0.32	0.29	0.3	0.38	0.33	0.32	0.35	0.3
Yb	1.7	1.7	2.1	2	2	2.4	2.2	2.1	2.3	1.9
Lu	0.25	0.28	0.33	0.31	0.31	0.37	0.34	0.34	0.35	0.29
Hf	2.9	3.3	4.3	3.9	4.1	4.9	3.6	3.7	4.3	4
Ta	0.3	0.5	0.8	0.5	0.7	1	0.4	0.4	0.6	0.6
W	276	380	572	324	290	101	442	371	221	376
Tl	<i>b.d</i>	<i>b.d</i>	<i>b.d</i>	<i>b.d</i>	<i>b.d</i>	<i>b.d</i>	<i>b.d</i>	<i>b.d</i>	<i>b.d</i>	<i>b.d</i>
Bi	<i>b.d</i>	<i>b.d</i>	<i>b.d</i>	<i>b.d</i>	<i>b.d</i>	<i>b.d</i>	<i>b.d</i>	<i>b.d</i>	<i>b.d</i>	<i>b.d</i>
Th	2.7	2.5	3.5	3.5	3.8	2.3	2.2	2.2	2.4	1.9
U	0.8	0.9	1.1	1.1	1.2	0.7	0.6	0.6	0.7	0.5

Trace-element compositions were determined using inductively coupled plasma mass spectrometry (ICP-MS) at Activation Laboratories, Ontario, Canada

b.d. below detection limit

Table S2. Measured FeO wt% from titrations using the Wilson (1960) method

Sample	Titration 1 wt% FeO	Titration 2 wt% FeO	Average FeO wt%	± 1 σ	± 2 σ
BP-7	6.81	6.57	6.69	0.17	0.34
BP-8	5.71	5.66	5.69	0.04	0.07
¹ BP-11	5.28	4.97	5.13	0.22	0.44
BP-16	6.36	5.64	6.00	0.51	1.02
BP-19	6.09	6.23	6.16	0.10	0.20
BP-20	6.18	5.84	6.01	0.24	0.48
BP-23	6.22	6.43	6.33	0.15	0.30
BP-24	5.73	5.74	5.74	0.01	0.01
BP-30	5.92	6.02	5.97	0.07	0.14
BP-31	6.20	6.18	6.19	0.01	0.03

	Titration 1 wt% FeO	Titration 2 wt% FeO	Average FeO wt% ± 1 σ	Average FeO wt% ± 1 σ for all W-2a measurements
² W-2a (10/05/19)	8.27	8.22	8.25 ± 0.04	8.44 ± 0.22
² W-2a (10/10/19)	8.61	8.64	8.63 ± 0.02	

¹BP-11 contains alteration products in its vesicles

²Two set of titrations were performed one week apart. Replications on USGS standard W-2a during a given session are presented with associated average ± 1 σ

Table S3. Standards employed for electron microprobe analyses of olivine, clinopyroxene, plagioclase, and Fe-Ti oxides

Standards employed for electron microprobe analyses of olivine		
Element (olivine)	Standard name (standard block)	Mineral name of the standard
Mg,Si	FOBO	Bolten forsterite
Fe	FESI	Ferrosilite (synthetic)
Ni	NiOI	Ni-olivine
Al	JADE	JD-1 Jadeite
Mn	BHRH	Rhodonite (Broken Hill)
Cr	Cr2O3	Cr ₂ O ₃ (Synthetic)
Ca	WOLL	Wollastonite (ANU)
Standards employed for electron microprobe analyses of clinopyroxene		
Element (clinopyroxene)	Standard name (standard block)	Mineral name of the standard
Mg	ENST	Enstatite (Harvard, H131709)
Na	JADE	JD-1 Jadeite
Si	GKFS	Adularia (St. Gothard)
Al	JADE	JD-1 Jadeite
Fe	FESI	Ferrosilite (synthetic)
Ni	NiOI	Ni-olivine
Cr	Cr2O3	Cr ₂ O ₃ (Synthetic)
Mn	BHRH	Rhodonite (Broken Hill)
Ti	GEIK	Geikelite (Synthetic)
Ca	WOLL	Wollastonite (ANU)
Standards employed for electron microprobe analyses of plagioclase		
Element (plagioclase)	Standard name (standard block)	Mineral name of the standard
Mg	GEIK	Geikelite (Synthetic)
Na	TAB	Albite (Tiburion)
Si	GKFS	Adularia (St. Gothard)
Al	TANZ	Tanzanite
Ti	GEIK	Geikelite (Synthetic)
Fe	FESI	Ferrosilite (synthetic)
Mn	BHRH	Rhodonite (Broken Hill)
Ca	WOLL	Wollastonite (ANU)
K	GKFS	Adularia (St. Gothard)
Standards employed for electron microprobe analyses of Fe-Ti oxides		
Element (Fe-Ti oxides)	Standard name (standard block)	Mineral name of the standard
Mg	GEIK	Geikelite (Synthetic)
Ca,Si	WOLL	Wollastonite (ANU)
Al	TANZ	Tanzanite
Cr	CR2O3	Cr ₂ O ₃ (Synthetic)
V	V2O5	V ₂ O ₅ (Synthetic)
Fe	Mag USNM	Magnetite (Minas Gerais, NMNH 114887)
Mn	BHRH	Rhodonite (Broken Hill)
Ti	Ilm USNM	Ilmenite (Ilmen Mountains, NMNH 96189)